Crustal characteristics beneath the Tien Shan belt, Central Asia, using seismic receiver function and potential field investigations

By Sattam Almadani

Crustal characteristics beneath the Tien Shan belt, Central Asia, using the seismic receiver function

Sattam A. Almadani

Department of Geology and Geophysics, college of Science, King Saud University, Riyadh, Saudi Arabia.

Corresponding author: Sattam Almadani; E-mail: salmadani@ksu.edu.sa; Tel: 966 11 4673515; Fax: 966 11 467 3662

Abstract

Globally, the Tien Shan belt is one of the most active seismic zones. The crustal structure beneath this belt was evaluated using teleseismic waveforms from 20 broadband stations covering the entire belt, as well as gravity modeling. The crustal thickness varies from 36 km to 68 km where the crust thickens due north and the southwest of Tien Shan, while the central part has a thin crust. The area of interest has V_p/V_s ratio of 1.81 ± 0.025 , indicating a mafic crust, detached by Moho from the mantle. Additionally, collision zone between Tien Shan and the Tarim Basin has the thickest crust and highest Φ values. The average Moho sharpness, R (0.17), is comparable to that of the typical crust and decreases due northwest. Stations near the Naryn Basin thin crust of about 42 km, probably due to delamination of the lower crust.

Key words: crustal structure, Moho, Vp/Vs ratio, receiver function, Tien Shan

1. Introduction

The Tien Shan mountains belt is located in Central Asia and oriented E-W. It is 2500 km long, 300-500 km width, with elevation of 7000 m (Molnar and Tapponnier, 1975). Recently, Tien Shan belt have a considerable earthquake activity where earthquakes with magnitudes greater than 8 have been recorded in this century (Molnar and Deng, 1984; Deng et al., 2000). Bump and Sheehan (1998) observed that earthquakes that take place in southern Tien Shan are mainly shallow (10-20 km), whereas those

occurring on the northern side originate at depths of 40 km or deeper. Most earthquakes occur near the border fault zones and in the active faults within the mountain belt (Avouac et al., 1993). Therefore, it is a great example and provides significant information concerning the deformation of mountain building. Tien Shan has always been a subject of debate among scholars. Although several researchers investigate mantle structure, they have not studied the composition and structure of the crust underneath (Tapponnier and Molnar, 1979; Vinnik et al., 1984; Vinnik and Saipbekova, 1984; Lukk et al., 1995; Bumb and Sheehan, 1998; Zhiwei et al., 2009).

Vinnik and Saipbekova (1984) used arrival times to calculate P wave travel-time residuals and concluded that there is a low wave speed in the uppermost mantle underneath Tien Shan. Assuming that the thickness of the crust varies linearly with mean elevation. They found a crustal thickness ranging from 55-60 km, by using data from 14 seismometers in central and western Tien Shan. Vinnik et al. (2006) stated that the crustal thickness is greatest (about 60 km) in the intersection of Tarim Basin and Tien Shan. They also detected that the crust-mantle boundary in this region changes rapidly because of an increasing thickness of lower crust. They applied the receiver functions inversion of P- and S-waves with teleseismic travel-time data. Yu et al. (2007) propose that the absence of a clear mountain root beneath Tien Shan, which implies that the material differentiation between the crust and mantle has not yet been accomplished and the orogenic development continues. By applying the arrival time tomography techniques, Zhiwet at al. (2009) declared the presence of thin lithosphere (less than 100 km depth) underneath the central part of Tien Shan and proposed the high wave-speed regions broaden from the surface to a depth of 400 km, or even deeper. Omuralieva et al. (2009) noticed a low-velocity zone due to the flow of mantle upwelling.

According to Gao et al. (2013), the crustal structure under Tien Shan and Tarim Basin was imaged on N-S-direction. Khan et al., (2017) studied the crustal structure of the Tien Shan orogenic belt and its neighboring provinces and suggested reverse-faulting earthquakes control the area of interest.

Chen et al. (1997) have proposed that the Tien Shan may be characterized by lithosphere activity. They came to this conclusion based on the delay times of the Ps converted phases beneath the region. Bump and Sheehan (1998) revealed the crustal thickness ranges between 37 km to 60 km in north-central Tien Shan using receiver function analysis. They used teleseismic events between 30° and 90° with magnitudes greater than 6.0. They also observed that in general, the crust thickens with increasing elevation. Deyuan et al. (2000) revealed a two-layer crustal structure, namely the lower and upper crusts, based on deep seismic sounding profiling.

2. Regional Tectonics

Tectonically, the Tien Shan is situated between the active Tarim Basin from the south and from north by stable Kazakh Shield (Fig. 1). Tien Shan is dominated by an E-W trending structure with 10-15 mm/yr and 2-6 mm/yr reducing rate of southern and northern Tien Shan respectively (Buslov et al., 2004). The current topography is mainly a result of uplift in Cenozoic time in response to the India-Eurasia collision (Peltzer and Trapponnier, 1988; Burchfiel and Royden, 1991; Yin et al., 1998). Strike-slip and normal fault types (Omuralieva et al., 2008) characterize most of the Tien Shan area. Geological studies related to timing and sequences have proposed the distortion of Tien Shan initiated 20 Ma after Indo-Asian collision (Abdrakhmatov et al., 2002). Furthermore, geologists stated that the Tien Shan has stayed tectonically inactive for most of the Late Cretaceous and Cenozoic (Burtman et al., 1996).

3. Data

The used dataset through this study include teleseismic waveforms recorded by 20 broadband stations belonging to the networks of XW (16 stations), KN (AML and ULHL), II (AAK), and G (WUS). They were requested from data management center at IRIS and were recorded from August 1997 to August 2010 with epicentral distances ranging from 30° to 180° (Fig. 2). These data consist of three-component seismograms with a clear P-wave arrival. The seismograms were filtered between the frequency range of 0.05 Hz and 1.5 Hz. Finally, more than 1424 radial receiver functions were chosen.

4. Receiver Function Analysis

Receiver function analysis is a robust method used to determine the Earth's crustal structure (Langston, 1977; Vinnik, 1977; Clouser and Langston, 1995; Liu et al., 2003; Gao et al., 2004; Liu and Gao, 2006 and 2010). It utilizes the teleseismic earthquakes waveforms, recorded by three components seismometer, to image the crustal structures beneath isolated seismic stations. The processing sequence detects the crustal/mantle boundary through recognizing P-to-S converted waves and their multiples from the Moho. Primary conversion (PmS or Ps) and multiple phases (PPmS, also called PpPs and PSmS, also referred as PpSs) often be recognized. Multiples phases are weaker than the Ps wave and consequently they are sometimes hard to recognize (Yuan et al., 2002). Crustal thickness and the average V_p/V_s ratio can be estimated through the identification of the crustal multiples (Zhu and Kanamori, 2000). Whereas, the V_p/V_s ratio is a valuable measure of crustal composition (using its relation to Poisson's ratio) (Zandt et al., 2004; Behn and Kelemen, 2006).

The procedure of Zhu and Kanamori (2000) H-k stacking technique was applied through this study, where H denotes the Moho depth and Φ is V_p/V_s ratio. A series of depths, H_i , varies between 15 and 55 km for Afar and 35-75 km for Tien Shan with 0.1 km, and Φ_j from 1.70 to 2.10 for Afar and 1.65 to 1.95 for Tien Shan, increases of 0.0025 were used. The moveouts of PmS, PPmS, and PSmS were estimated for each (H_i , Φ_i) following Nair et al. (2006) method. The following equations (1-4) were used for PmS, $t_1^{(i,j)}$ estimation:

$$t_1^{(i,j)} = \int_{-H_i}^0 \left[\sqrt{(V_p(z)/\phi_j)^{-2} - p^2} - \sqrt{V_p(z)^{-2} - p^2} \right] dz \tag{1}$$

Where p represents P-wave ray, H_i refers the depth discontinuity, Φ_j denotes V_p/V_s , and $V_p(z)$ is the velocity of P wave at depth z.

moveouts, t2(i,j) of PPmS assessed by:

$$t_2^{(i,j)} = \int_{-H_i}^0 \left[\sqrt{(V_p(z)/\phi_j)^{-2} - p^2} + \sqrt{V_p(z)^{-2} - p^2} \right] dz$$
 (2)

and those of PSmS, t₃^(i,j), were:

$$t_3^{(i,j)} = \int_{-H_i}^0 2\sqrt{(V_p(z)/\phi_j)^{-2} - p^2} dz$$
 (3)

For each station, the receiver functions were stacked as:

$$A(H_i, \phi_j) = \sum_{k=1}^n w_1 S_k(t_1^{(i,j)}) + w_2 S_k(t_2^{(t,j)}) - w_3 S_k(t_3^{(i,j)})$$
(4)

The weighting factors w_1 , w_2 , and w_3 in this study were set for both areas to 0.5, 0.3, and 0.2, respectively. A reference crustal velocity $V_{p(z)}$ of 6.3 km/s was chosen for the Afar Depression and Tien Shan. Position's ratio (σ) was calculated following Christensen, (1996) formula. To estimate the standard deviations of the resulting parameters, the bootstrap method (Efron and Tibshirani, 1986; Press et al., 1992) has been applied in this study. The abovementioned procedures were attained using the computer programs developed aby Geophysical group at Missouri S&T (Gao et al., 2002; Liu et al., 2003; Gao et al., 2004; Liu and Gao, 2006; Liu and Gao, 2008).

5. Results

The results were categorized into category A displaying stations with strong single peak and consequently H and k are identified. The crustal thickness (H_n) has been estimated with Φ of 1.80, which is approximately the mean Φ of Category A stations in the study area. Most receiver functions display a comprehensible peak of H-k plot. Category A stations include (ARA, KAZ, DGE, KARL, TERE, KASH, HARA, WUS, KSA, and AKSU) where most of stations of this groups presents precise crustal thickness. The crustal thickness underneath these stations ranges from 36.1 km (KAZ) to 68 km (HARA). The values of Φ ranges from 1.724 at DGE to 1.85 at HARA. The R-value range from 0.098 (AKSU) to 0.336 (KASH). While category B stations include (AML, AAK, KAI, ULHL, ANA, AHQI, KENS, KOPG, KAR, and POGR). The stations

are described by crustal thickness in the range of 46 km (KAI and KOPG) to 65.7 km (ANA) and R values between 0.084 (ULHL) and 0.267 (KOPG).

The crustal thickness varies in a range from 36 km (east of the Talas Fergana fault) to about 68 km (northwestern corner of the Tarim Basin). The crust thickens in the north and the southwest side of Tien Shan, while the central part has a thin crust. The crustal thickness beneath KAZ is among the smallest in the region (36.1 km), Φ =1.84 and R =0.281. The northwestern corner of the Tarim Basin, beneath HARA, shows the thickest crust, highest Φ , and average R-values. In most cases, the crustal thickness values increase from north to south with increasing elevation. ARA, DGE, KARL, HARA, and KSA show a well-defined crustal thickness and normal Moho amplitude. The Moho can be clearly noticeable even on individual receiver functions. Most of the stations in this study show well pronounced PmS.

6. Discussions

The crustal thickness determined from the method of receiver function analysis in this study shows an average of 53 km. The crustal thickness varies from 36 km easting of Talas Fergana Fault to 68 km in the northwestern corner of Tarim Basin. We observed that the crust is much thicker in the north and the southwest; however, it is quite thin in the central part of Tien Shan. Our calculated values are consistent with earlier geophysical determinations, which suggested a similar crustal thickness from P- and S-receiver functions (Oreshin, 2002). Bump and Sheehan (1998) used receiver functions analysis and obtained measurements of crustal thickness at AAK and AML. They observed large variations with back azimuth at AAK and minimal changes in depth with back azimuth at AML. In general, there are increasing in the crustal thickness southward with increasing elevation. Northwestern corner of the Tarim Basin (HARA) shows the thickest crust, highest Φ , and average R-values. The crustal thickness beneath KAZ is among the smallest (36.1 km), Φ (1.84) and R (0.281). ARA, DGE, KARL, HARA, and KSA stations show a well-defined crustal thickness.

The results of the crustal thickness for AAK and AML are close to the results of Bump and Sheehan (1998). They found that the crustal thicknesses beneath these two stations are 51 km and 60 km respectively (Table 1). The H measurements, from this study, are correlated well with those obtained by Bump and Sheehan (1998), with a difference of a few kilometers. We observed that the crustal thickness values increase to the south towards TERE, HARA, and KASH, with increasing station elevation. The largest crustal thickness (68 km) is found in the Tarim-Tien Shan junction zone and is possibly under-thrusting. These explanations are in agreement with those mentioned by Scharer et al. (2004).

The H-k method offers an estimation of average crustal V_p/V_s that can be converted directly into the Poisson's ratio. Our interpretation based on V_p of 6.3 km/s. Lying on the foundation of 76 universal examples, Zandt and Ammon (1995) proposed that the V_p/V_s ratio generally rises with the age of the crust. They found that Mesozoic-Cenozoic belts are regularly still tectonically active, with extensive surface relief and crustal thickness variations. The V_p/V_s distribution in this study is, in fact, rational all over the study area. Stations TERE, HARA, and KASH at the northwestern corner of the Tarim Basin have high values of V_p/V_s up to 1.85, with the highest in the entire study area at HARA (1.85). It seems that the observed Φ values in this area, to some extent, are related to crustal thickness. For example, the crust beneath HARA has the highest values of Φ and H. Most of the category A stations have high values of Poisson's ratio ranging from (0.24-0.29), indicating the presence of intermediate mafic components in the crust.

The results of this study suggest variations in the stacking amplitude (R) beneath the stations. The average resulting R (0.17) is similar to that of typical crust and decreases towards the northwest. The depths of Moho at AML, ARA, and KAI relatively with constant depth. From TERE through KASH, the Moho depth increases towards the junction zone between Tarim Basin and southern Tien Shan, indicating that the Moho is deepening and agreeing with a previous study by Vinnik et al. (2004), which showed crustal thickening beneath this region.

7. Conclusions

Tien Shan belt presents higher V_p/V_s ratios and higher amplitude stacking below almost stations indicating isolated mafic crust. Central Tien Shan is mostly different from southern and the northern parts in terms of crustal thickness and Moho sharpness. Additionally, the collision zone between Tien Shan and Tarim Basin leading to the thickest crust and highest Φ values. The thickest crust of 68 km recorded below Tarim Basin. In most cases, crustal thickness increases from north to south, with increasing elevation. The average resulting R (0.17) is similar to the typical crust and decreases towards the northwest. Stations near the Naryn Basin present thin crust of about 42 km.

1 Acknowledgments

The authors would like to extend their sincere appreciation to the Deanship of Scientific Research at King Saud University for its funding this research group No. RGP -1436-010.

References

- Abdrakhmatov KY, Weldon R, Thompson S, Burbank D, Rubin C, Miller M, Molnar P (2002) Origin, direction, and rate of modern compression of the Central Tien Shan. Geology and Geophysics (Russian) 42(10), 1585–1609.
- Allen M, Vincent SJ and Wheeler PJ (1999) Late Cenozoic tectonics of the Kepingtage thrust zone: interactions of the Tien Shan and Tarim Basin northwest China. Tectonics, 18, pp. 639–654.
- Avouac J P and Tapponnier P (1993) Active Thrusting and Folding Along the Northern Tien Shan and Late Cenozoic Rotation of the Tarim Relative to Dzungaria and Kazakhstan. Journal of Geophysical Research, v. 98, n. B4. pp. 6755-6804.
- Bump H A and Sheehan A F (1998) Crustal thickness variations across the northern Tien Shan from teleseismic receiver functions. Geophysical Research Letters, v. 25, n. 7, pp. 1055-1058.
- Burchfiel BC and Royden LH (1991) Tectonics of Asia 50 years after the death of Emile Argand, Eclogae Geol. Helv. 84, pp. 599–629.

- Burchfiel BC, Brown ET, Deng Q, Feng X, Molnar J Li P, Shi J, Wu Z and You H (1999). Crustal shortening on the margins of the Tien Shan, Xinjiang, China. Int. Geol. Rev., 41 (1999), pp. 665–700.
- Buslov MM, Grave JD, and Bataleva E A (2004) Cenozoic tectonics and geodynamic evolution of the Tien Shan Mountain belt as response to India-Eurasia convergence. Himalayan Journal of Sciences, v. 2, Issue. 4.
- Buslov MM, Fujiwara Y, Iwata K, Semakov N (2004) Late Paleozoic–Early Mesozoic geodynamics of Central Asia. Gondwana Research, 7, 791–808.
- Deng QD, Feng XY, Zhang PZ, Xu XW, Yang XP, Peng SZ, Li SZ, J. (2000). Active Tectonics of the Chinese Tian Shan Mountains. Seismology Press, Beijing (in Chinese with English Abstract).
- Deyuan L, Qiusheng L, Rui G, Yingkang L, Dexing L, Wen L, and Zhiying Z (2000). A deep seismic sounding profile across the Tianshan Mountains. *Chinese Science Bulletin*, Vol. 45 No. 22.
- Konopelko D, Biske G, Seltmann R, Kiseleva M, Matukov D, and Sergeev S (2008)
 Deciphering Caledonian events: timing and geochemistry of the Caledonian magmatic arc in the Kyrgyz Tien Shan. Journal of Asian Earth Sciences, 32 (2–4), 131–141.
- Konopelko D, Biske G, Seltmann R, Eklund O, and Belyatsky B (2007) Hercynian postcollisional A-type granites of the Kokshaal Range, Southern Tien Shan, Kyrgyzstan. Lithos, 97, 140–160.
- Lukk AA, Yunga S L, Shevchenko V I, and Hamburger M W (1995) Earthquake focal mechanisms, deformation state, and seismotectonics of the Pamir-Tien Shan region, central Asia, J. Geophys. Res., 100, 20,321 – 20,343, 1995.
- Molnar P and Tapponnier P (1975) Cenozoic tectonics of Asia; effects of continental collision. Science 189, 419–426.
- Molnar P and Tapponnier P (1981) A possible dependence of tectonic strength on the age of the crust in Asia. Earth and Planet. Sci. Lett., 52, 107-114.
- Molnar P and Deng Q (1984) Faulting associated with large earthquakes and the average rate of deformation in central and eastern Asia: Journal of Geophysical Research, v. 89, p. 6203–6227.

- Neil EA, Houseman GA (1997) Geodynamics of the Tarim Basin and the Tian Shan in Central Asia. Tectonics, 16(4), 571–584.
- Omuralieva A, Nakajima J, and Hasegawa A (2009) Three-dimensional seismic velocity structure of the crust beneath the central Tien Shan, Kyrgyzstan: Implications for large-and small-scale mountain building. Tectonophysics, 465 (2009) 30–44.
- Peltzer G, Topponnier P, Gaudemer Y and Meyer B (1988) Offsets of late Quaternary morphology, rate of slip, and recurrence of large earthquakes on the Chang Ma fault (Gansu, China), J. Geophys. Res., 87, pp. 7793–7812.
- Reigber C, Michel GW, Galas R, Angermann D, Klotz J (2001) New space geodetic constraints on the distribution of deformations in Central Asia, Earth Planet. Sci. Lett., 191 (2001) 157–165.
- Sobel ER and Dumitru TA (1997) Thrusting and exhumation around the margin of the western Tarim basin during India–Asia collision. J. Geophys. Res., 102, pp. 5043–5063.
- Tapponnier P and Molnar P (1979) Active faulting and Cenozoic tectonics of the Tien Shan. Journal of Geophysics Research. Vol. 48, No. B7.
- Vinnik LP, Aleshin I M, Kaban M K, Kiselev S G, Kosarev G L, Oreshin S I, and Reigber Ch (2006) Crust and Mantle of the Tien Shan from Data of the Receiver Function Tomography. Physics of the Solid Earth, 2006, Vol. 42, No. 8, pp. 639–651.
- Vinnik LP, and Saipbekova A M (1984) Structure of the lithosphere and asthenosphere of the Tien Shan, Annales Geophysicae, 2, 621 626.
- Yin A, Nie S, Craig P, Harrison TM, Ryerson FJ, Qian X and Yang G (1998). Late Cenozoic tectonic evolution of the southern Chinese Tian Shan, Tectonics 17 (1998), pp. 1–27.
- Zhiwei L S, Roecker L, Zhihai W, Bin W, Haitao G, Schelochkov Bragin V(2009) Tomographic image of the crust and upper mantle beneath the western Tien Shan from the MANAS broadband deployment: Possible evidence for lithospheric delamination. Tectonophysics, 477, 49–57.

Figure captions
Figure 1: Surface topography of the Tien Shan including: the distribution of seismic stations [blue triangles], earthquakes [red stars], and existing faults [green
lines]. Figure 2: Locations of the events used in the Tien Shan
11

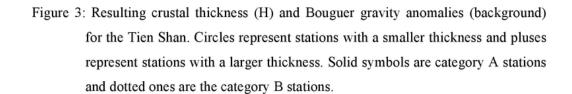


Table Captions

Table 1: Table of comparison with previous crustal thickness results for the Tien Shan.

Crustal characteristics beneath the Tien Shan belt, Central Asia, using seismic receiver function and potential field investigations

ORIGINALITY REPORT						
9% SIMILARITY INDEX PRIMARY SOURCES						
				1	mdpi.com Internet	28 words — 1 %
				2	www.coursehero.com Internet	22 words — 1 %
3	link.springer.com Internet	22 words — 1 %				
4	iugg.org Internet	21 words — 1%				
5	eaton.math.rpi.edu	16 words — 1 %				
6	Yu Li, QiYuan Liu, JiuHui Chen, ShunCheng Li, Biao Guo, YuanGen Lai. "Shear wave velocity structure of the crust and upper mantle underneath the tianshan or Science in China Series D: Earth Sciences, 2007 Crossref	15 words — 1 % ogenic belt",				
7	www.tandfonline.com Internet	14 words — 1 %				
8	Alzoman, Nourah, Maha Sultan, Hadir Maher, Mona 12 Alshehri, Tanveer Wani, and Ibrahim Darwish. "Analytical Study for the Charge-Transfer Complexes of Rosuvastatin Calcium with π-Acceptors", Molecules, 20	of				

Crossref

- Buslov, M.M.. "Cenozoic tectonic and geodynamic evolution of the Kyrgyz Tien Shan Mountains: A review of geological, thermochronological and geophysical data", Journal of Asian Earth Sciences, 20070201
- Ilya V. Sychev, Ivan Koulakov, Nailia A. Sycheva, Alexander Koptev, Irina Medved, Sami El Khrepy, Nasir Al-Arifi. "Collisional Processes in the Crust of the Northern Tien Shan Inferred From Velocity and Attenuation Tomography Studies", Journal of Geophysical Research: Solid Earth, 2018
- Delores M. Robinson. "The Tula uplift, northwestern 10 words < 1% China: Evidence for regional tectonism of the northern Tibetan Plateau during late Mesozoic—early Cenozoic time", Geological Society of America Bulletin, 01/2003
- Lianghui Guo, Rui Gao, Lei Shi, Zhangrong Huang, Yawei Ma. "Crustal thickness and Poisson's ratios of South China revealed from joint inversion of receiver function and gravity data", Earth and Planetary Science Letters, 2019
- M.E. Bullen. "Late Cenozoic tectonic evolution of the northwestern Tien Shan: New age estimates for the initiation of mountain building", Geological Society of America Bulletin, 12/2001
- Zhiwei, L.. "Tomographic image of the crust and upper mantle beneath the western Tien Shan from the MANAS broadband deployment: Possible evidence for lithospheric delamination", Tectonophysics, 20091101
- Huang, B.. "Paleomagnetism of Miocene sediments from the Turfan Basin, Northwest China: no significant vertical-axis rotation during Neotectonic compression within the Tian Shan Range, Central Asia", Tectonophysics, 20040616

- Jianshe Lei. "Seismic tomographic imaging of the crust and upper mantle under the central and western Tien Shan orogenic belt", Journal of Geophysical Research, 09/16/2011
- Mikhail K. Kaban, T. Reiza Yuanda. "Density Structure, Isostatic Balance and Tectonic Models of the Central Tien Shan", Surveys in Geophysics, 2014

EXCLUDE QUOTES
EXCLUDE
BIBLIOGRAPHY

ON

ON

EXCLUDE MATCHES

< 5 WORDS